UNCLASSIFIED

SECURITY CLASSIFICATION OF THIS PAGE

ADA200652

REPORT DOCUMENTATION PAGE

1a. REPORT SECURITY CLASSIFICATION UNCLASSIFIED	1b. RESTRICTIVE MARKINGS
2a. SECURITY CLASSIFICATION AUTHORITY	3. DISTRIBUTION/AVAILABILITY OF REPORT
2b. DECLASSIFICATION/DOWNGRADING SCHEDULE	
4. PERFORMING ORGANIZATION REPORT NUMBER(S) FJSR1-JR-88-0011	5. MONITORING ORGANIZATION REPORT NUMBER(S)
6a. NAME OF PERFORMING ORGANIZATION Frank J. Seiler Research Lab 6b. OFFICE SYMBOL (If applicable) FJSRL/NH	7a. NAME OF MONITORING ORGANIZATION
6c. ADDRESS (City, State and ZIP Code) USAF Academy Colorado Springs, CO 80840-6528	7b. ADDRESS (City, State and ZIP Code)
8a. NAME OF FUNDING/SPONSORING ORGANIZATION 8b. OFFICE SYMBOL (If applicable)	9. PROCUREMENT INSTRUMENT IDENTIFICATION NUMBER
8c. ADDRESS (City, State and ZIP Code)	10. SOURCE OF FUNDING NOS. PROGRAM ELEMENT NO. 61102F; PROJECT NO.; TASK NO. 2301-F1; WORK UNIT NO. 72
11. TITLE (Include Security Classification) Intensity-dependent absorption and photorefractive effects in barium titanate (U)	
12. PERSONAL AUTHOR(S) George A. Brost, Raymond A. Motes, James R. Rotge'	
13a. TYPE OF REPORT Journal Publication 13b. TIME COVERED FROM _____ TO _____	14. DATE OF REPORT (Yr., Mo., Day) 88 Sep 15. PAGE COUNT 7
16. SUPPLEMENTARY NOTATION	

17. COSATI CODES			18. SUBJECT TERMS (Continue on reverse if necessary and identify by block number)
FIELD	GROUP	SUB. GR.	
2006	2012	2014	$BaTiO_3$, absorption coefficient, photorefractive, barium titanate

19. ABSTRACT (Continue on reverse if necessary and identify by block number)

We present experimental data for $BaTiO_3$ that exhibit an intensity dependence in the absorption coefficient and the two-beam coupling coefficient between 0.0002 and 40W/cm^2. The effective empty-trap concentration was found to increase with intensity. We present a model, in the spirit of commonly used (photorefractive) theories, for photorefraction and optical absorption that explains these effects. The intensity dependence was attributed to the presence of secondary photorefractive centers.

20. DISTRIBUTION/AVAILABILITY OF ABSTRACT UNCLASSIFIED/UNLIMITED ☐ SAME AS RPT. ☒ DTIC USERS ☐	21. ABSTRACT SECURITY CLASSIFICATION UNCLASSIFIED
22a. NAME OF RESPONSIBLE INDIVIDUAL Raymond A. Motes, Captain, USAF	22b. TELEPHONE NUMBER (Include Area Code) 719-472-3122 22c. OFFICE SYMBOL FJSRL/NH

DD FORM 1473, 83 APR EDITION OF 1 JAN 73 IS OBSOLETE.

UNCLASSIFIED

SECURITY CLASSIFICATION OF THIS PAGE

Reprinted from Journal of the Optical Society of America B, Vol. 5, page 1879, September 1988

Intensity-dependent absorption and photorefractive effects in barium titanate

G. A. Brost, R. A. Motes, and J. R. Rotge

Frank J. Seiler Research Laboratory, U.S. Air Force Academy, Colorado 80840

Received March 10, 1988; accepted May 25, 1988

We present experimental data for $BaTiO_3$ that exhibit an intensity dependence in the absorption coefficient and the two-beam coupling coefficient at intensities between 0.002 and 40 W/cm^2. The effective empty-trap concentration was found to increase with intensity. We present a model, in the spirit of commonly used (photorefractive) theories, for photorefraction and optical absorption that explains these effects. The intensity dependence was attributed to the presence of secondary photorefractive centers.

INTRODUCTION

Barium titanate ($BaTiO_3$) has been the subject of extensive research in recent years. Through the photorefractive effect, it is able to show high optical nonlinearities at low power levels and has been used for applications such as optical phase conjugation[1] and optical resonators.[2,3] The physical process involved in the photorefractive effect is a light-induced redistribution of charges among traps. The resulting space-charge field then modulates the refractive index through the linear electro-optic effect.

Although there has been much interest in the applications of the photorefractive effect, little is known regarding the species responsible for the effect in $BaTiO_3$. Previous research suggests that iron impurities are the primary sources and traps of the photorefractive charge carriers.[4,5] Models based on these deep traps provide a reasonably good understanding of the photorefractive effect but are yet incomplete.[6-9] For example, Motes and Kim found an intensity dependence in the absorption and two-beam coupling coefficients that is not explained by the current models.[10,11]

In this paper we examine the intensity-dependent absorption and photorefractive effects in $BaTiO_3$ and present a model in which the absorption characteristics are accounted for by the presence of secondary centers. These are intermediate-level traps that are highly ionized at room temperature and acquire free-charge carriers generated by the interaction of the laser light with deep-level impurities. We incorporate the secondary centers into a photorefractive model and show that they lead to intensity-dependent photorefractive effects not predicted by current models. Characteristics of these centers are discussed.

GENERAL BACKGROUND

The grating formation in a photorefractive material is commonly described by either the band-transport model[6,8] or the hopping model,[7] both of which give the same results. The band model is shown schematically in Fig. 1. The charge carriers may be either electrons or holes (or both). Photoconductivity in $BaTiO_3$ is usually hole dominated, and, for simplicity, we discuss the single-carrier model. X and X' constitute a complete set of recombination centers. Holes are photoionized from X and recombine at X'. Overall charge neutrality is maintained by other states that are not photorefractively active. Under illumination by sinusoidally modulated light, as from an interference pattern between two coherent optical beams, holes optically excited in the high-intensity regions migrate by diffusion and drift to the darker regions of the crystal, where they recombine with empty traps. This redistribution of charges results in an ionic space-charge grating that is out of phase with the periodic light-intensity pattern. The charge separation is balanced by a periodic space-charge electric field that is $\pi/2$ phase shifted with respect to the light intensity (no externally applied electric field). This space-charge field then modulates the refractive index through the electro-optic effect. The phase grating is also $\pi/2$ shifted with respect to the light intensity.

A mathematical description of the grating-formation process has been given by Kukhtarev *et al.*[6] for a light-intensity pattern resulting from the interference of two coherent beams I_S and I_P:

$$I(z) = I_0[1 + m \exp(iKz)], \tag{1}$$

where m is the modulation index given by $m = 2(I_S I_P)^{1/2} I_0$, $I_0 = I_S + I_P$, and K is the grating wave number. For small modulation index, the magnitude of the modulated space-charge field can be written as[4,5]

$$E_{SC} = R(mk_BT/q)\{K/[1 + (K/K_0)^2]\}, \tag{2}$$

where

$$K_0^2 = q^2 N_E/(\epsilon\epsilon_0 k_B T), \tag{3}$$

$$N_E = N_X(1 - N_X/N_X), \tag{4}$$

and

$$R = \sigma_p/(\sigma_p + \sigma_d). \tag{5}$$

Here k_B is Boltzmann's constant. T is the lattice temperature, q is the charge of a hole, ϵ is the dielectric constant, ϵ_0 is the permittivity of free space, N_X and $N_{X'}$ are the concentrations of the donors and traps, N_E is the effective empty-trap

0740-3224/88/091879-07$02.00

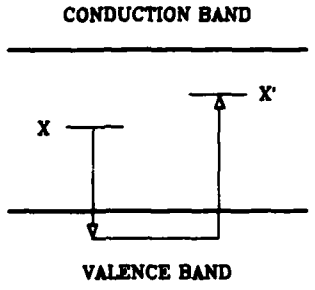

Fig. 1. Energy-level diagram of band model for photorefraction in $BaTiO_3$. Holes are photoionized from level X and recombine at X'.

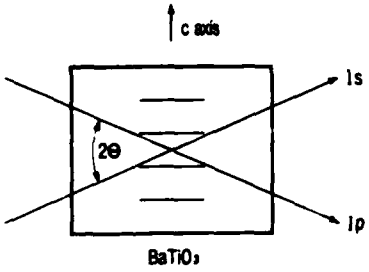

Fig. 2. Crystal orientation and beam notation for two-beam coupling in $BaTiO_3$.

concentration, and σ_d and σ_p are the dark conductivity and photoconductivity, respectively. The amplitude of the modulated refractive index n_1 is given by

$$n_1 = (1/2)n^3 r_{\text{eff}} E_{\text{SC}}, \tag{6}$$

where n is the index of refraction and r_{eff} is the effective electro-optic coefficient.

The grating formation in a photorefractive crystal is accompanied by an energy redistribution between the two interfering light beams that is due to the $\pi/2$ phase mismatch between the phase grating and the light-intensity pattern.[12,13] This two-beam coupling is shown schematically in Fig. 2. The two optical beams have transmitted intensities I_S and I_P, and the crystal c axis is chosen so that the signal beam (I_S) experiences gain defined as

$$\gamma_0 = \frac{I_S \text{ (with } I_P \text{ on)}}{I_S \text{ (with } I_P \text{ off)}}. \tag{7}$$

The amplitude gain can be expressed in terms of exponential gain coefficient[12,14] (Γ):

$$\gamma_0 = \frac{(1+\beta_0)\exp(\Gamma d)}{1+\beta_0 \exp(\Gamma d)}, \tag{8}$$

where d is the interaction length and the parameter β_0 is the intensity ratio of the two incident beams ($\beta_0 = I_{S0}/I_{P0}$). The exponential gain coefficient is related to the space-charge field by

$$\Gamma = kn^3 r_{\text{eff}} E_{\text{SC}}/m, \tag{9}$$

where k is the wave number of the laser light.

Equations (1)–(9) demonstrate that the exponential gain (two-beam coupling) coefficient is dependent on the trap concentration and the grating spatial frequency but has little dependence on the total light intensity. The only intensity dependence comes from the parameter R, which reflects the relative contributions of photoconductivities and dark conductivities. Except at low intensities, where the photoconductivity is small, R is approximately equal to 1. Therefore the steady-state photorefractive effect is frequently described as being independent of laser intensity.[1,5,8,15]

Despite strong interest in the applications of $BaTiO_3$ there is a dearth of information pertaining to its photorefractive characteristics and, in particular, its intensity-dependent effects. Experiments are frequently conducted at intensities of 10–100 mW/cm^2, where the photoconductivity dominates the dark conductivity.[4,9] Townsend and LaMacchia[16] and later Rak *et al.*[17] found an intensity dependence in the photorefractive effect in $BaTiO_3$ that saturated at approximately 1 W/cm^2, but they did not investigate it in any detail. They attributed the intensity dependence to a diffraction efficiency that was proportional to the steady-state concentration of free carriers. This model is not supported by current photorefractive theories and does not explain other aspects of the photorefractive effect. More recently, Motes and Kim[10,11] reported an intensity dependence in the optical absorption coefficient as well as in the two-beam coupling coefficient. They showed that the intensity dependence in the photorefractive effect varied with spatial frequency and was responsible for an asymmetry in the coupling coefficient with respect to the c-axis direction.

EXPERIMENT

Although the experimental data of Motes and Kim[11] clearly showed an intensity dependence in the absorption and photorefractive two-beam coupling, their photorefractive data were scattered, and comparison with theoretical results was inconclusive. We therefore repeated those measurements on a p-type $BaTiO_3$ crystal that was electrically poled. The $BaTiO_3$ crystal was grown by Sanders Associates and was used as grown. These nominally undoped crystals typically contain large concentrations of transition-metal impurities. Klein and Schwartz[5] recently completed an extensive study of the impurities present in $BaTiO_3$ (grown by Sanders) and found that iron was the dominant impurity, with concentrations of 50–150 parts in 10^6 (ppm).

The intensity-dependent absorption in $BaTiO_3$ is characterized by an absorption coefficient that increases with laser intensity. The intensity-dependent portion of the absorption coefficient, α_I, can be defined as the difference between the absorption coefficient measured at high intensity, α_H, and that measured at low intensity, α_0, ($\alpha_I = \alpha_H - \alpha_0$). We measured α_I by using the experimental arrangement shown in Fig. 3. We used the 514-nm line of an argon-ion laser. The power of a weak signal beam (I_S) was monitored by a photodetector. For the absorption measurements, the path difference between the pump (I_P) and the signal beam was made much greater than the coherence length to eliminate mutual photorefractive effects. We also used ordinary polarization to reduce the effects of self-induced photorefractive effects. In the presence of I_P, I_S was reduced owing to the intensity-dependent absorption. We determined α_I by using the relation

$$\frac{I_S \text{ (with } I_P \text{ on)}}{I_S \text{ (with } I_P \text{ off)}} = \exp(-\alpha_I d), \tag{10}$$

where d is interaction length.

The experimental results are shown in Fig. 4. The varia-

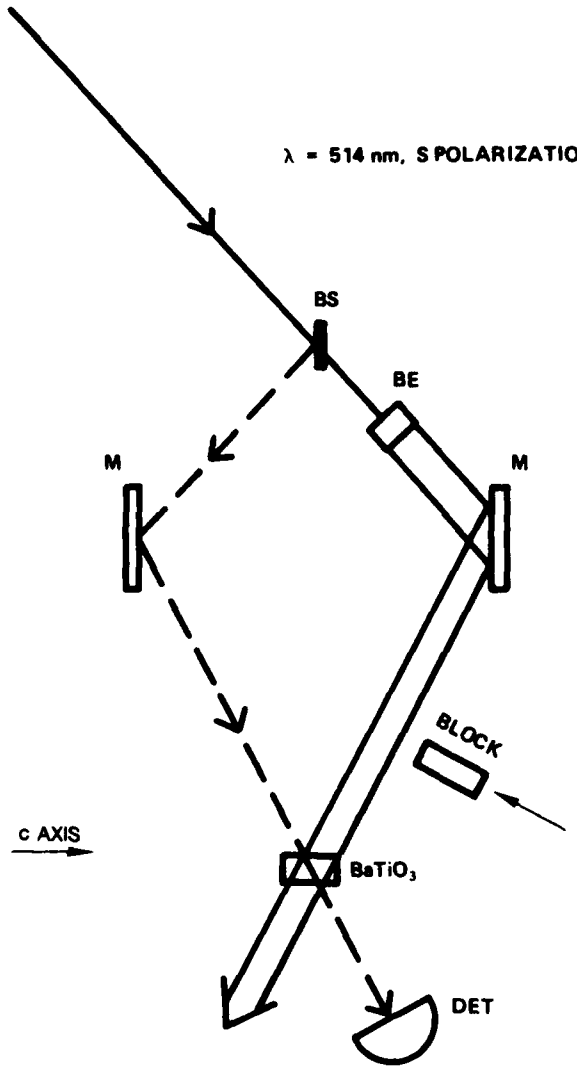

Fig. 3. Experimental arrangement for intensity-dependent measurements in $BaTiO_3$: BE, beam expander; BS, beam splitter; DET, detector; M's, mirrors. For absorption measurements, the path difference between I_P and I_S was made much greater than the coherence length.

tion in the absorption coefficient begins to be observed at cw intensities less than 0.1 W/cm^2 and saturates at approximately 20 W/cm^2. The intensity-dependent absorption appears to be a common characteristic of $BaTiO_3$, as it has been observed in all eight crystals that we have tested.

The intensity dependence of the exponential gain coefficient was measured by using the experimental arrangement shown in Fig. 3. Two coherent beams of an argon-ion laser, operating at 514 nm,were aligned so that the direction of the grating wave vector was parallel to the c axis of the $BaTiO_3$ crystal. The beams were polarized to become ordinary rays. The pump beam was expanded by a 2× beam expander to ensure overlap between the two laser beams, and the intensity of the signal beam was much less than the pump-beam intensity ($\beta_0 = 0.05$). In this geometry the signal beam I_S experiences an increase in intensity as described by Eqs. (7) and (8). When intensity-dependent absorption is present, the right-hand side of Eq. (8) should be multiplied by the factor $\exp(-\alpha_I d)$.[10]

A plot of the gain coefficient corrected for absorption versus grating period for different pump-beam intensities is shown in Fig. 5. An increase in beam intensity is seen to result in an increase in the magnitude of the gain coefficient and a shift in the peak of the curve to smaller grating periods. Although an intensity dependence can be attributed to the effects of dark conductivity, this cannot fully explain the features observed in Fig. 5. The intensity-dependent characteristics due to dark conductivity are manifested in Eq. (5). The coupling coefficient should increase with intensity from a small value and should level off at intensities at which the photoconductivity dominates the dark conductivity. The small change in the magnitude of Γ between the two lower intensity curves would indicate that the dark conductivity is not dominating the photoconductivity in this intensity range. The large increase in Γ in going to yet higher intensities is not characteristic of a dark-conductivity effect. Also, as seen from the equations developed in the previous section, the intensity dependence due to dark conductivity should be independent of grating period. The intensity dependence seen in Fig. 5 is more consistent with a change in the trap concentration. This point will be discussed in more detail below.

SECONDARY PHOTOREFRACTIVE CENTERS

The observed intensity dependences in the absorption and photorefractive effect are not in agreement with the models that are currently used to describe photorefraction in

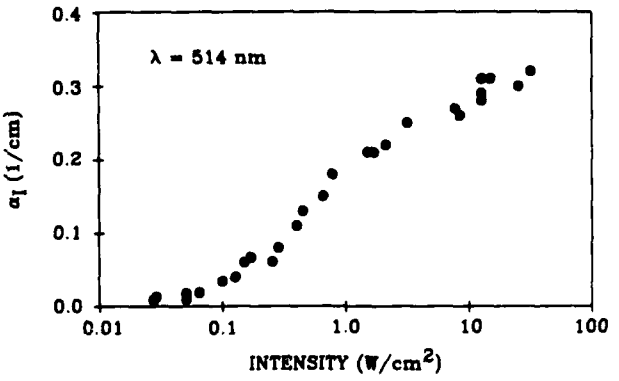

Fig. 4. Experimental values of intensity-dependent absorption coefficient α_I versus laser intensity in $BaTiO_3$.

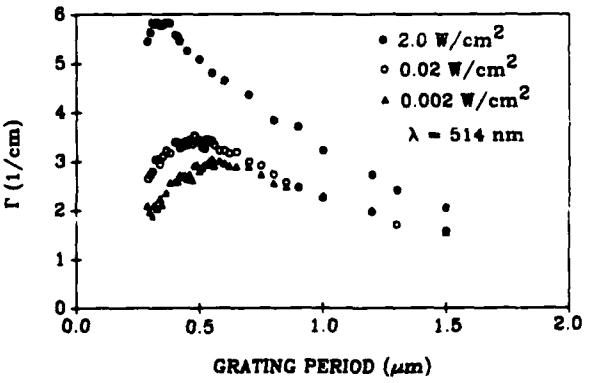

Fig. 5. Measured two-beam coupling coefficient (Γ) corrected for absorption versus grating period for different laser intensities.

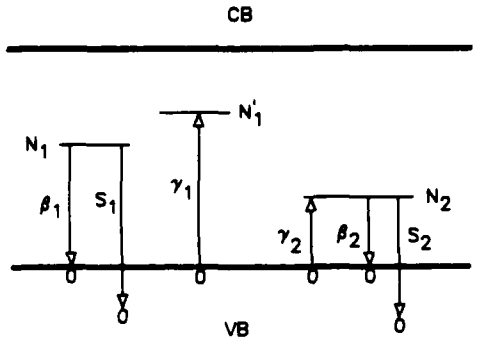

Fig. 6. Schematic diagram of the secondary-center model for $BaTiO_3$. N_1 and N_1' are primary photorefractive centers, and N_2 is the secondary photorefractive center. CB, conduction band; VB, valence band.

$BaTiO_3$. In this section we show that the inclusion of secondary photorefractive centers in the band model accounts for the intensity-dependent effects.[18]

The physical mechanisms responsible for the intensity-dependent absorption in $BaTiO_3$ have not previously been identified. Motes *et al.*[9] have shown that this is not a photorefractive effect. It exists in unpoled crystals, can be induced at one wavelength and observed at a second wavelength, and has a rise time of the induced absorption that is an order of magnitude faster than the grating-formation time. The effect is observed at low intensities, ruling out two-photon absorption. Thermal effects are not responsible. This is shown by the decrease in absorption with increasing temperature[11] and the fast time response of the induced absorption.[19] Apparently either an absorption mechanism is being created or an existing mechanism is being enhanced. Most models used to describe the photorefractive effect in $BaTiO_3$ consider only the interactions with primary photorefractive centers—deep traps among which charge is redistributed. These models cannot account for the intensity-dependent absorption at intensities of 0.1–10 W/cm^2. We suggest that the intensity-dependent absorption is due to secondary photorefractive centers that exist in addition to the deep traps. These are traps that are shallower than the primary centers and strongly ionized. At low laser intensity, there is, therefore, no measurable absorption due to the secondary centers. At higher laser intensities these traps begin to fill with holes generated in photoabsorption by the deep traps. Provided that the thermal ionization rate is not too high and that the absorption cross section is larger than that for the deep traps, an enhancement in the absorption coefficient will be observed. These secondary centers can also be expected to influence the photorefractive characteristics in the same intensity range.

A model that incorporates the secondary centers is shown schematically in Fig. 6. This is a modification of the band model. N_1 and N_1' constitute a single set of recombination centers (presumably Fe^{3+} and Fe^{2+}, respectively). Holes are photoionized from N_1 and recombine at N_1'. The photoionization of N_1 is taken to result in the formation of an N_1', and, similarly, the hole recombination with an N_1' forms an N_1. In addition to these primary photorefractive centers, secondary photorefractive centers are present and are denoted by N_2. The identity and characteristics of N_2 are yet unknown, and, for simplicity, we show only one energy level.

The occupation levels for N_1 and N_2 are described by the rate equations

$$dN_1/dt = -(S_1 I + \beta_1)N_1 + \gamma_1(N_{1T} - N_1)N_h, \quad (11)$$

$$dN_2/dt = -(S_2 I + \beta_2)N_2 + \gamma_2(N_{2T} - N_2)N_h, \quad (12)$$

where S_1 and S_2 are the photon-absorption cross sections, γ_1 and γ_2 are the recombination coefficients, β_1 and β_2 are the thermal ionization rates, I is the laser intensity, N_{2T} and N_{1T} are the total concentration of species N_2 and N_1, and N_h is the concentration of free carriers (holes). $(N_{2T} - N_2)$ is the concentration of secondary photorefractive centers that are unoccupied, and $N_{1T} = N_1' + N_1$. We include a continuity, current, and Poisson equation, respectively, for completeness:

$$\partial N_h/\partial t = -dN_1/dt - dN_2/dt - \nabla \cdot j, \quad (13)$$

$$\mathbf{j} = N_h \mu \mathbf{E} - \frac{\mu k_B T}{q} \nabla N_h, \quad (14)$$

$$\nabla \cdot \mathbf{E} = (N_h + N_1 + N_2 - N_A)q/\epsilon\epsilon_0, \quad (15)$$

where μ is the hole mobility, $N_A = N_1(0) + N_2(0) + N_h(0)$, and $N_1(0)$, $N_2(0)$, and $N_h(0)$ are the dark concentrations. $N(0)$ reflects the dark conductivity, and its inclusion provides the associated intensity dependence expressed in Eq. (5), as discussed above. Overall charge neutrality is maintained by the presence of other impurities (e.g., oxygen vacancies).

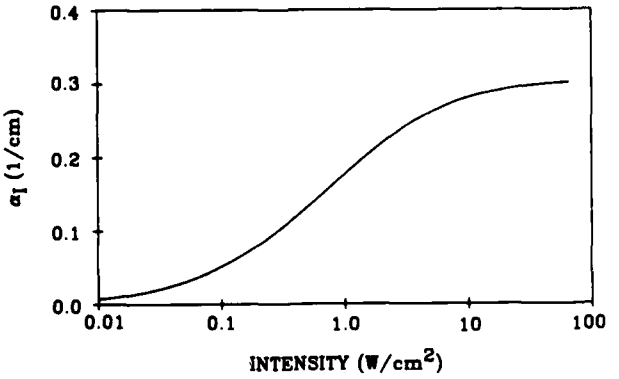

Fig. 7. Calculated intensity-dependent absorption coefficient versus laser intensity.

Table 1. Parameter Values Used in the Calculations[a]

Parameter	Value
S_1	2.5×10^{-19} cm^2
S_2	5×10^{-18} cm^2
γ_1	5×10^{-8} cm^3 sec^{-1}
γ_2	2.5×10^{-8} cm^3 sec^{-1}
β_1	1.5×10^{-4} sec^{-1}
β_2	30 sec^{-1}
N_{1T}	2.6×10^{18} cm^{-3}
$N_1(0)$	2.57×10^{18} cm^{-3}
N_{2T}	1.5×10^{17} cm^{-3}
$N_2(0)$	3.8×10^{13} cm^{-3}
$N_h(0)$	3×10^{5} cm^{-3}

[a] For the choice of the values see the Discussion section.

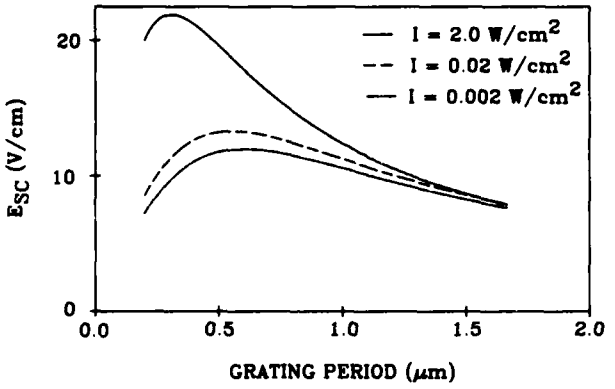

Fig. 8. Calculated space-charge field (E_{SC}) versus grating period for different intensities.

To calculate the intensity dependence in the absorption coefficient, we assumed a uniform laser intensity, set the electric field and current equal to zero, and solved for steady-state conditions. This resulted in a set of three equations [(11), (12), and (15)] and three unknowns (N_1, N_2, and N_h). These equations did not reduce to a convenient analytical form and were solved numerically. The intensity-dependent part of the absorption coefficient was then given by

$$\alpha_I = S_1[N_1 - N_1(0)] + S_2[N_2 - N_2(0)]. \quad (16)$$

Figure 7 shows the calculated steady-state values of α_I as a function of laser intensity for the parameter values listed in Table 1. The theoretical results exhibit rise and saturation characteristics similar to the experimental data. This increase in absorption reflects the photoenhanced population of secondary centers. At low-intensity illumination the secondary centers are populated by capture of free carriers, but thermal ionization dominates, and there is little change in the steady-state concentration compared with dark conditions. As the intensity increases, free carriers are photogenerated from the deep traps at a higher rate and fill the secondary traps at a rate comparable with the thermal ionization rate. The concentration of occupied secondary centers increases; therefore the absorption coefficient increases because of the high-absorption cross section of the secondary centers. At yet higher intensities, the secondary centers begin to fill up, and photoionization limits the occupied-trap concentration. The intensity region over which this transition takes place depends on all the parameters: absorption cross sections, recombination coefficients, and, most critically, thermal ionization rate.

To calculate the steady-state space-charge field we used a modulated intensity distribution given by Eq. (1). We assumed that $m \ll 1$ and solved for the lowest Fourier component of the grating by writing the variables as zeroth- and first-order terms:

$$N_1 = N_{10} + N_{11}\exp(iKz), \quad (17)$$

$$N_2 = N_{20} + N_{21}\exp(iKz), \quad (18)$$

$$N_h = N_{h0} + N_{h1}\exp(iKz), \quad (19)$$

$$E = E_0 + E_{SC}\exp(iKz), \quad (20)$$

$$j = j_0 + j_1\exp(iKz). \quad (21)$$

E_0 and E_{SC} correspond to the applied electric field and induced space-charge field, respectively. We considered only the diffusion problem where E_0 and j_0 were zero. Solution for the steady state proceeded by substituting Eqs. (17)–(21) into Eqs. (11)–(15) and keeping only zeroth- and first-order terms. This yielded a set of coupled nonlinear equations in the zeroth-order terms that were solved numerically for N_{10}, N_{20}, and N_{h0}, which were then used as parameters for the set of linear equations in the first-order terms. These equations were then solved numerically for E_{SC} as well as for N_{11}, N_{21}, and N_{h1}.

Figure 8 shows the calculated dependence of E_{SC} on grating period and intensity for the parameter values listed in Table 1. At low laser intensity few secondary centers are occupied, and the secondary-center model gives the same result as the Kukhtarev model. As the intensity increases, the steady-state concentration of secondary centers (N_2) also increases. This in turn results in an increase in the effective empty-trap concentration. Consequently the magnitude of the space-charge field is enhanced, and the peak is shifted to smaller grating periods. Although the secondary centers are traps, which are present even at low intensities, they do not contribute to the space-charge field until they are occupied with charge. Trapping of a hole by a secondary center also influences the concentration distribution of primary centers. If secondary centers are not present, the steady-state concentrations of N_1 and N_1' remain essentially unchanged from their initial values. But each hole trapped by a secondary center results in a decrease in the N_1 concentration and an increase in the N_1' concentration. Therefore the increase in the effective empty-trap concentration is given approximately by $2[N_2 - N_2(0)]$.

The effect of the secondary centers is more complicated than a simple increase in the number of participating traps. For a given grating period the magnitude of E_{SC} is proportional to the magnitude of the modulation in the ionic space charge (i.e., $N_{11} + N_{21}$). Although the modulation of N_1 was always dephased 180° with respect to the light-intensity sinusoid, the modulation in N_2 was found to be either in phase or 180° out of phase, depending on intensity and grating period. In general, for low intensities N_2 was in phase and at higher intensities and shorter grating periods N_2 was out of phase with the light intensity. For the results shown in Fig. 8, N_2 was in phase for the two lower-intensity curves, and at 2 W/cm², N_2 was out of phase for grating periods of less than 0.36 μm. The enhanced space-charge field at small grating periods was due primarily to an increase in N_{11}, which dominated N_{21}. As the grating period increased, the magnitude of N_{11} decreased, whereas N_{21} increased. At a grating period of 1.65 μm, the space-charge field was only slightly enhanced at an intensity of 2 W/cm² over that at 0.002 W/cm², despite an increase in the value of N_{11} by a factor of 4. This was because the increase in N_{11} was offset by the modulation in N_2. We applied the model to other parameter values and intensities but found no combination that allowed N_{21} to become greater than N_{11} and thereby to reverse the sign of the coupling.

DISCUSSION

Values for the various parameters used in this model are not well known, particularly for the secondary centers. The

values listed in Table 1 were chosen to be consistent with our data and the current understanding of $BaTiO_3$, as discussed below. These values do not necessarily represent a best fit to the data. There are too many parameters for which more-detailed knowledge is required to justify such an analysis.

Iron impurities are thought to be the primary photorefractive centers in $BaTiO_3$ and are usually present in concentrations of approximately 100 ppm (5×10^{18} cm^{-3}), with an Fe^{2+} to-Fe^{3+} ratio of approximately 0.01 for p-type crystals.[5] We estimated the N_1' (Fe^{2+}) concentration by using the effective empty-trap concentration of 2.6×10^{16} cm^{-3}, as determined from the two-beam coupling data at low intensity. We then took $N_1(0)$ to be 100 times this value. Klein and Schwartz[5] determined impurity concentrations and absorption coefficients at 442 nm for several $BaTiO_3$ crystals. From their data we estimated the absorption cross section for N_1 to be approximately 2.5×10^{-19} cm^2 at 514 nm. The recombination coefficient is thought to be approximately 5×10^{-8} cm^3/sec, consistent with a free-carrier lifetime of approximately 1 nsec.[8] The deep traps have a low thermal ionization rate, which is reflected in long grating-storage times. We used the value 1.5×10^{-4} sec^{-1} to be consistent with a finite dark level of carriers.

Characteristics of the secondary centers can be obtained through interpretation of the intensity-dependent absorption and photorefractive data. The increase in the effective empty-trap density inferred from the two-beam coupling data implies an increase in the occupied secondary-center concentration of approximately 4×10^{16} cm^{-3} at 2 W/cm^2. This can be combined with the intensity-dependent absorption data to give an absorption cross section of approximately 5.25×10^{-18} cm^2. The increase in occupied-secondary-center concentration saturated at approximately 6×10^{16} cm^{-3}. This suggests that the total concentration of secondary centers (N_{2T}) was approximately 1×10^{17} to 2×10^{17} cm^{-3}. We have estimated the thermal-ionization rate to be between 20 and 100 sec^{-1}, based on the temporal decay of the intensity-dependent absoprtion. This provides only an approximate value because the measured decay time is strongly influenced by the recombination coefficients and concentrations of N_1 and N_2. We find that a value between 20 and 40 sec^{-1} best reflects our absorption data.

The secondary center, N_2, is thus characterized as a highly ionized trap with a moderate thermal-ionization rate. The presence of such an impurity is not in conflict with the known defect chemistry of $BaTiO_3$. As-grown crystals are generally p type and are characterized by a high dark resistivity of 10^{11}–10^{16} Ω cm and therefore a low free-carrier concentration in the dark.[20-22] Although $BaTiO_3$ normally contains a high concentration of transition-metal impurities and barium vacancies that act as acceptors, a high concentration of oxygen vacancies is usually present, which compensates for the acceptor level, even when grown in a slightly oxidizing environment.[5,20]

We have not included photoabsorption by the N_1' impurity states. Besides providing centers for hole recombination, N_1' may also provide a center for electron photoexcitation. This process has recently been considered as a source for electron–hole competition in photorefraction.[23,24] In p-type $BaTiO_3$, in the absence of secondary traps, this absorption mechanism has negligible effect on the intensity-dependent absorption at the low laser intensities considered here. Much-higher intensities would be required to change the concentrations of N_1 and N_1'. However, as discussed above, when secondary centers are present, the concentration of N_1' is increased along with the concentration of occupied secondary traps. By neglecting absorption due to N_1', we have effectively assumed that the absorption cross section S_1' is small compared with S_2 and have attributed all the enhanced absorption to the secondary centers. If absorption by N_1' is important, then our conclusions about the characteristics of the secondary centers, such as the value of the recombination coefficient and the absorption cross section, would need to be modified accordingly. However, the essential feature of the model would be unaffected. The number of secondary centers involved, as indicated by the photorefractive data, would still be the same. Secondary traps would still be necessary to contribute to charge redistribution in either case. We have examined the case of electron traps populated through absorption by N_1'. Although these traps could account for the intensity-dependent absorption, the secondary hole traps were still necessary to account for the intensity-dependent photorefractive effects.

The secondary-center model presented here was intended to reflect conditions appropriate for p-type $BaTiO_3$. As such, the calculations were limited to hole production and a single-carrier photorefractive model. Our objective was to provide a basis for understanding the intensity-dependent effects in $BaTiO_3$. Extension of the model to include multiple secondary traps, both electron and hole, and mixed conductivity is straightforward. However, extension to a more elaborate model would also require additional parameters for which there is little or no knowledge.

CONCLUSION

We have attributed the intensity-dependent absorption and photorefractive effects in $BaTiO_3$ at cw laser intensities to the presence of secondary photorefractive centers. These are intermediate-level traps that are not completely occupied at room temperature and compete for charge carriers photoionized from the deep traps. The increase in the occupied concentration with higher laser intensity results in an enhanced absorption coefficient. The secondary centers also play a role in photorefraction by providing an intensity-dependent trap concentration.

REFERENCES AND NOTES

1. J. Feinberg in *Optical Phase Conjugation*, R. A. Fisher, ed. (Academic, New York, 1983).
2. P. Yeh, J. Opt. Soc. Am. B **2**, 1924 (1985).
3. J. O. White, M. Cronin-Golomb, B. Fischer, and A. Yariv, Appl. Phys. Lett. **40**, 450 (1982).
4. S. Ducharme and J. Feinberg, J. Opt. Soc. Am. B **3**, 283 (1986).
5. M. B. Klein and R. N. Schwartz, J. Opt. Soc. Am. B **3**, 293 (1986).
6. N. V. Kukhtarev, V. B. Markov, S. G. Odulov, M. S. Soskin, and V. L. Vinetskii, Ferroelectrics **22**, 949 (1979).
7. J. Feinberg, D. Heiman, A. R. Tanguay, Jr., and R. W. Hellwarth, J. Appl. Phys. **51**, 1297 (1980).
8. G. Valley and M. Klein, Opt. Eng. **22**, 704 (1983).
9. M. B. Klein and G. Valley, J. Appl. Phys. **57**, 4901 (1985).
10. A. Motes and J. J. Kim, Opt. Lett. **12**, 199 (1987).
11. A. Motes and J. J. Kim, J. Opt. Soc. Am. B **4**, 1379 (1987).
12. P. Gunter, Phys. Rep. **93**, 199 (1982).
13. D. Staebler and J. Amodei, J. Appl. Phys. **43**, 1042 (1972).
14. A. Marrakchi and J. P. Huignard, Appl. Phys. **24**, 131 (1981).

15. J. P. Huignard and G. Rosen, in *Nonlinear Optics: Materials and Devices*, C. Flytzanis and J. L. Oudar, eds. (Springer-Verlag, Berlin, 1986).
16. R. L. Townsend and J. T. LaMacchia, J. Appl. Phys. **41**, 5188 (1970).
17. D. Rak, I. Ledoux, and J. P. Huignard, Opt. Commun. **49**, 302 (1984).
18. C. Chen, D. M. Kim, and D. Von der Linde, IEEE J. Quantum Electron. **QE-16**, 126 (1980). The term secondary photorefractive center was used here to describe enhanced effects in $LiNbO_3$ under pulsed illumination.
19. A. Motes, G. Brost, J. Rotgé, and J. Kim, Opt. Lett. **13**, 509 (1988).
20. A. M. J. H. Seuter, Philips Res. Rep. Suppl. **3**, 1 (1974).
21. S. Ducharme and J. Feinberg, J. Appl. Phys. **56**, 839 (1984).
22. E. Kratzig, F. Welz, R. Orlowski, V. Doorman, and M. Rósenkranz, Solid State Commun. **34**, 817 (1980).
23. G. Valley, J. Appl. Phys. **59**, 3363 (1986).
24. F. P. Strohkendl, J. M. C. Jonathan, and R. W. Hellwarth, Opt. Lett. **11**, 312 (1986).